Comparing Coastal Surface Circulation Statistics Derived From Altimetry and Imagery

Dax Matthews, Bill Emery, Dan Baldwin
University of Colorado, Boulder
Colorado Center for Astrodynamics Research

Abstract

Knowledge of ocean boundary currents is necessary to develop a quantitative understanding of the kinetic energy budget of the coastal region and to give a more accurate oceanographic forecast. This is of great interest to both ocean industry (shipping and oil) and ocean research. Surface currents off the California coast from north of San Francisco to south of Los Angeles are calculated using sequential thermal infrared images from the Advanced Very High Resolution Radiometer (AVHRR), combined with altimeter data from the Jason-1, Topex/Poseidon, GFO, and ERS-2 satellites. A Maximum Cross Correlation (MCC) technique is used to identify motion of the thermal patterns which act as tracers of the surface current. Altimeter data is used to compute geostrophic surface currents, which are then combined with the MCC velocities using Optimal Interpolation (OI) to produce a gridded stream function. The most critical steps to produce viable results are automatic geo-registration, cloud filtering, computations of the MCC currents, vector compositing, and the Optimal Interpolation technique. This poster examines the effects of different sampling configurations and methods on derived mesoscale ocean currents.

Maximum Cross Correlation (MCC) Technique

Velocities are estimated by tracking thermal patterns in successive 1 km AVHRR thermal infrared images. The first image is divided into subwindows (solid boxes) and each window cross correlated with subwindows in the search area of a second image (dashed boxes). The location that produces the maximum cross correlation (second image, solid boxes) indicates the most likely displacement of the features (shown by the vectors).

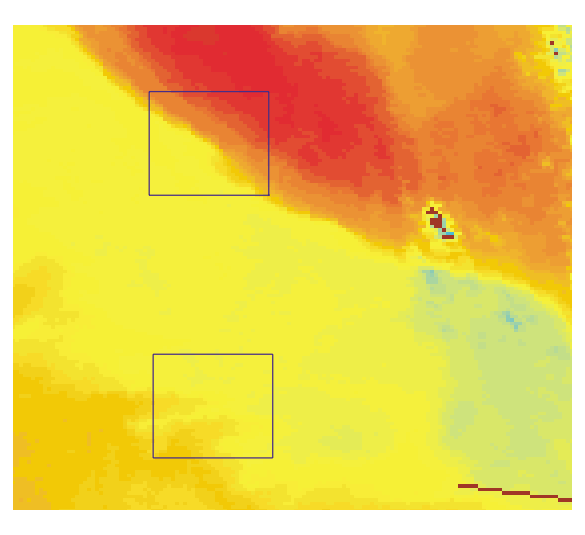
Image 1

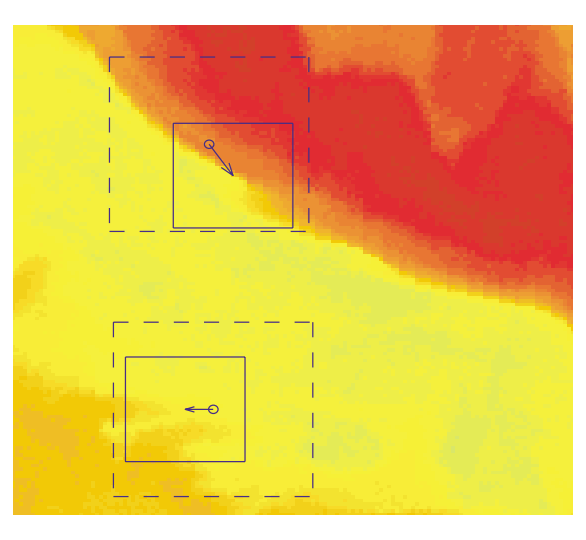
Image 2

Optimal Interpolation

The value of a stream function at every grid point is found using a weighted sum of altimeter sea surface heights and MCC velocities. The weights are determined by the choice of the covariance functions in space and time, the error and signal variances of the data, and the location and time of each observation relative to the grid point, with typical length scales of ~ 200 km and time scales of ~10 days (Bretherton et al 1976, LeTraon and Hernandez 1992). Interpolating the alimeter heights or the MCC velocites alone usually captures similar basic features. Merging combines the strengths of the two data sets.

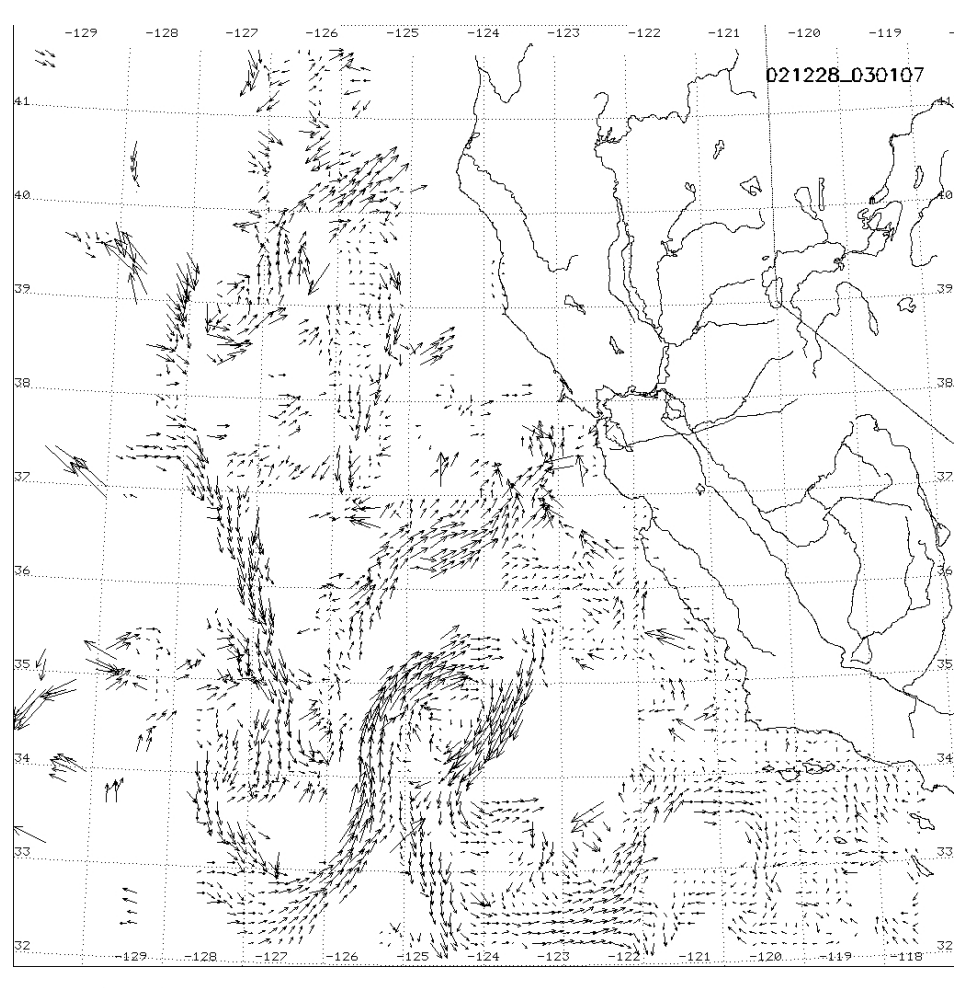

MCC Velocites

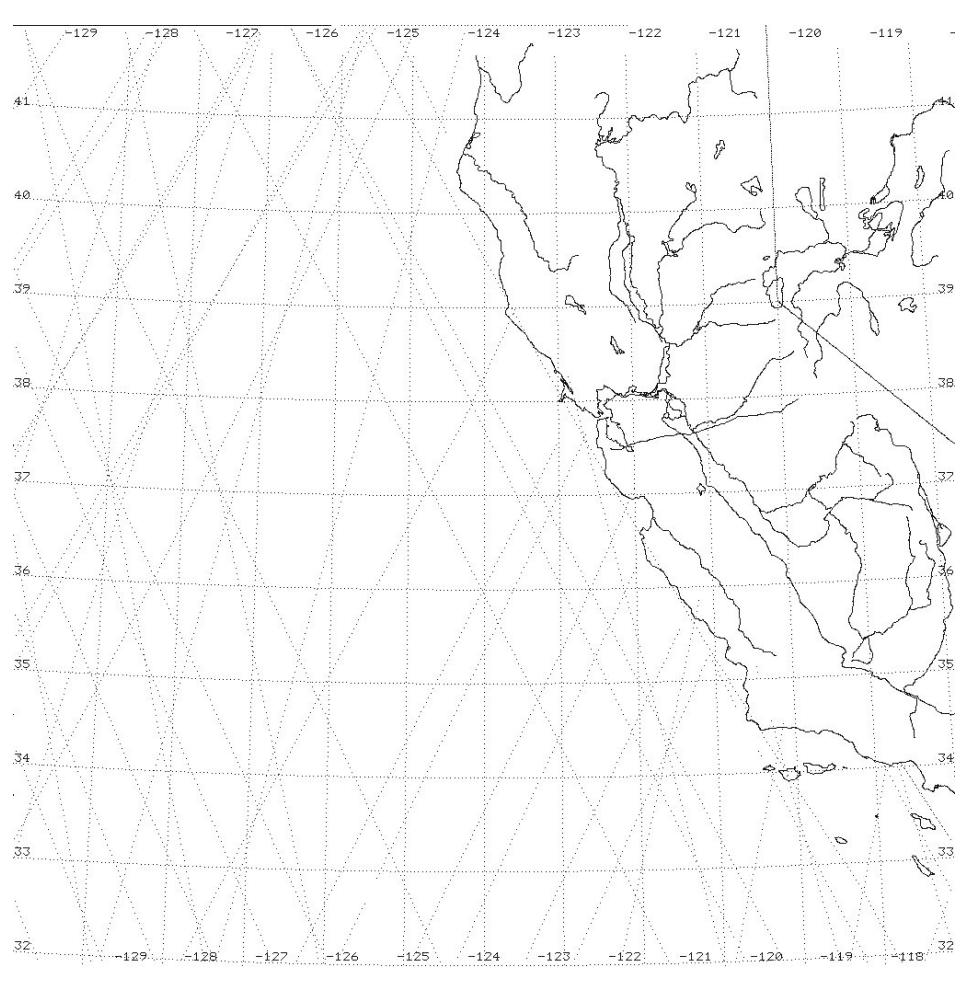
Altimeter Tracks

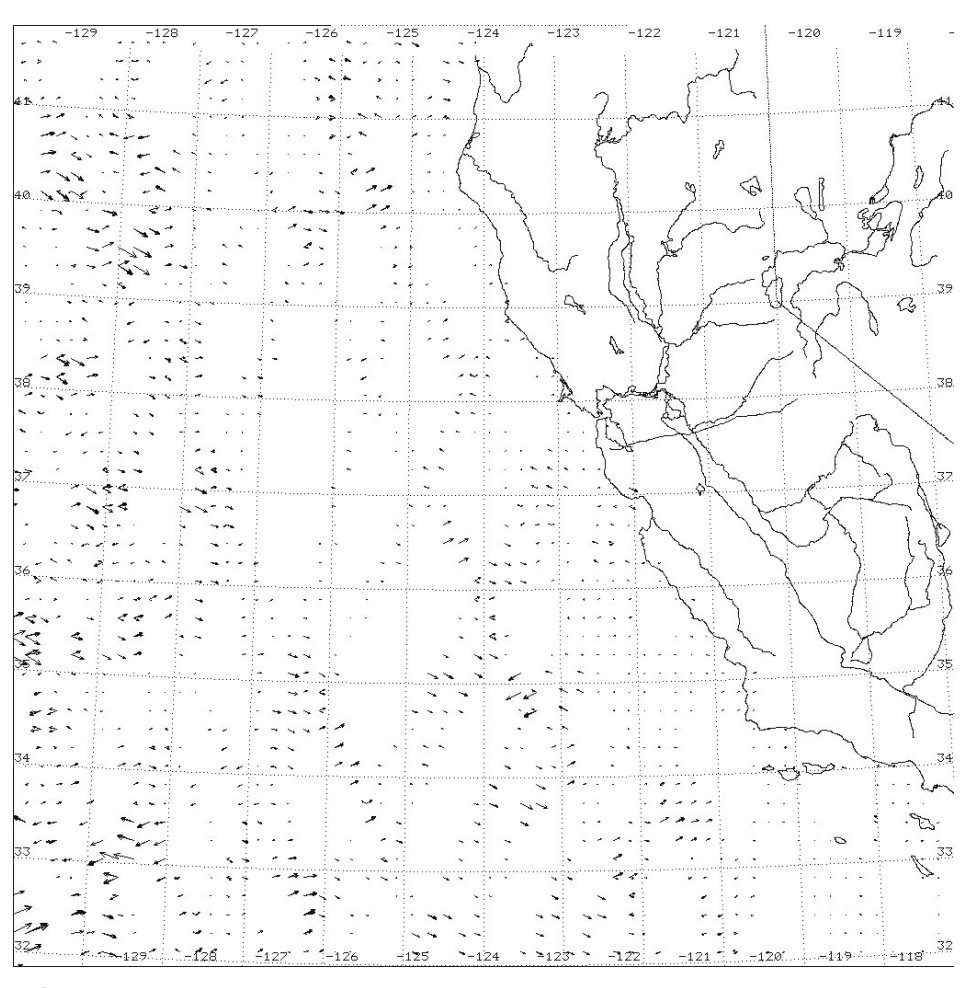
Geostrophic Velocites

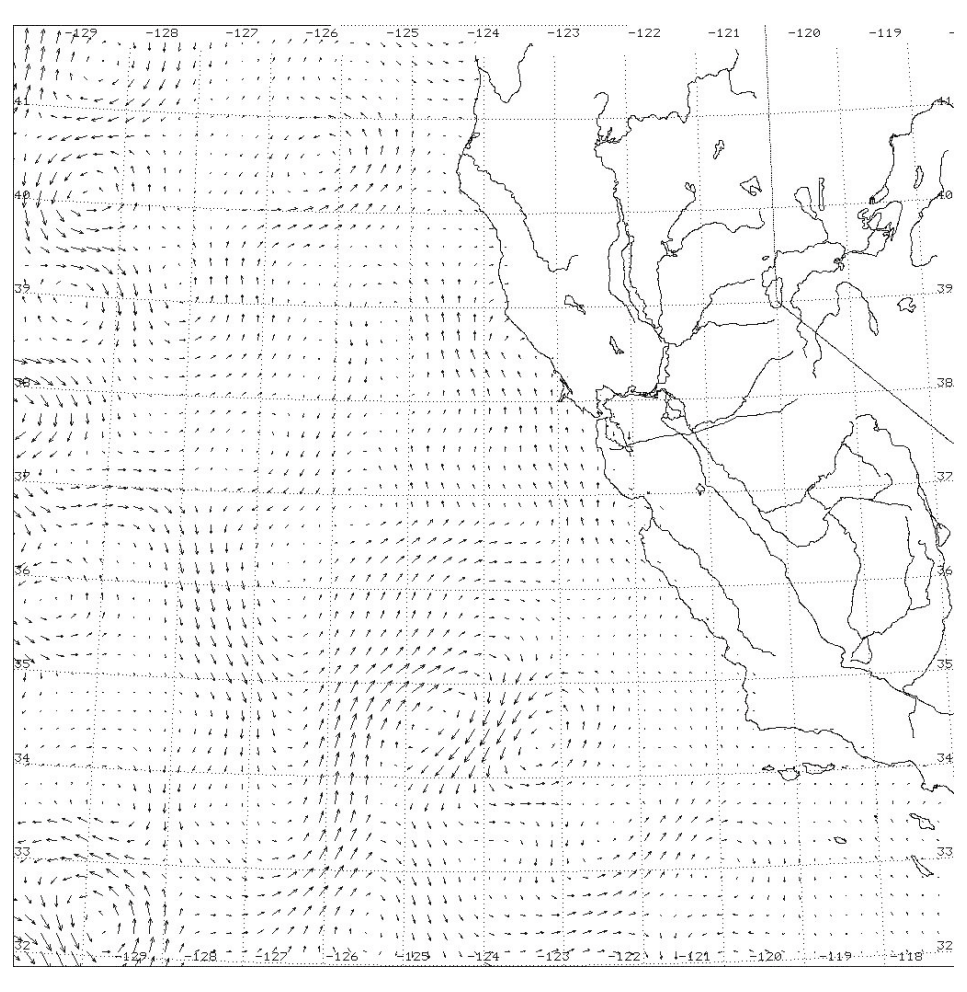
Combined OI Velocites

Observations

The Topex, Jason, GFO, and ERS2 altimeters measure sea surface height anomalies along widely-spaced but regular tracks at 10 or 35 day intervals (left panel). In regions such as the California Current the coarse spatial and temporal sampling is likely not to resolve the evolution of the mesoscale features properly.

Number of Vectors

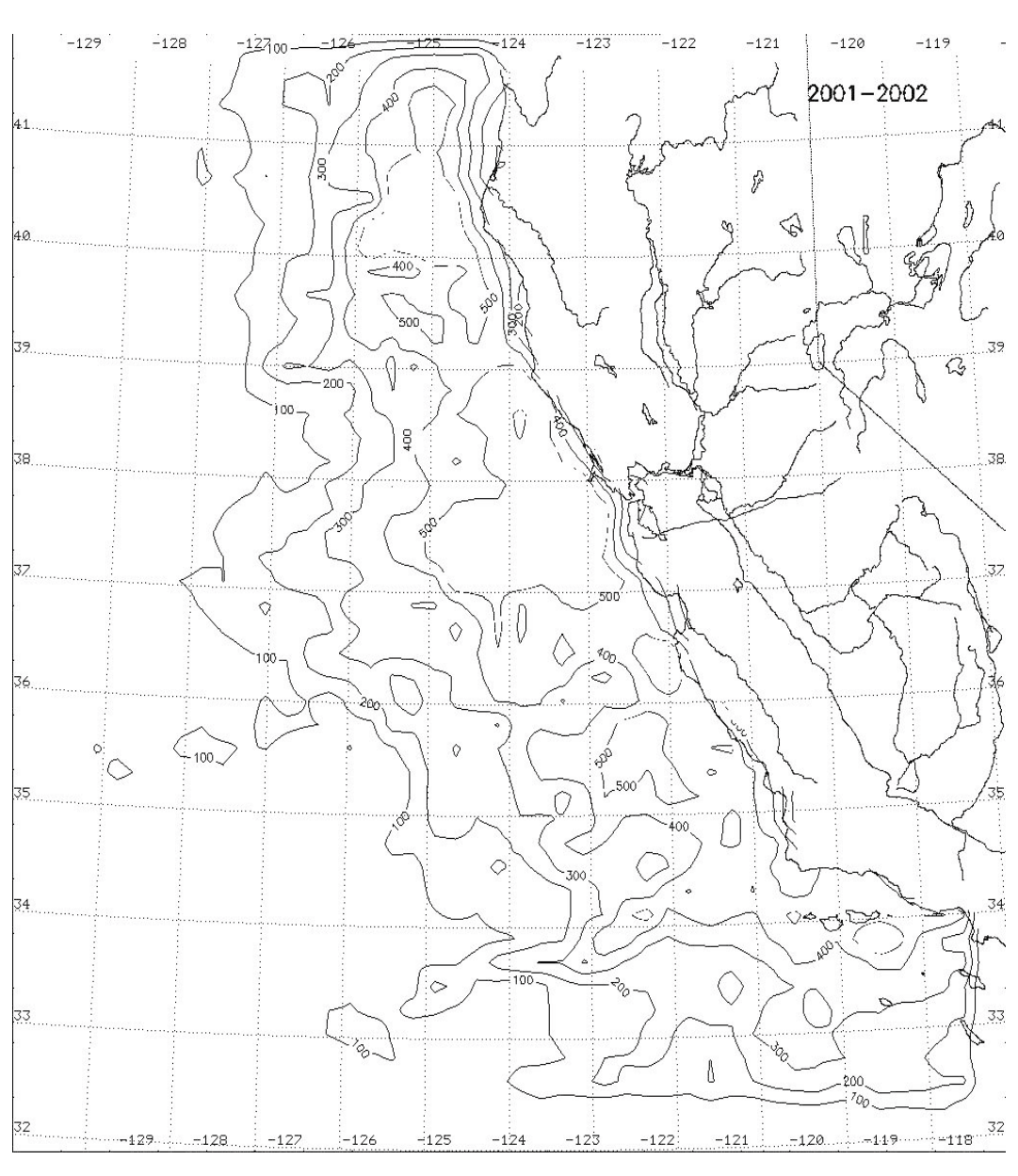

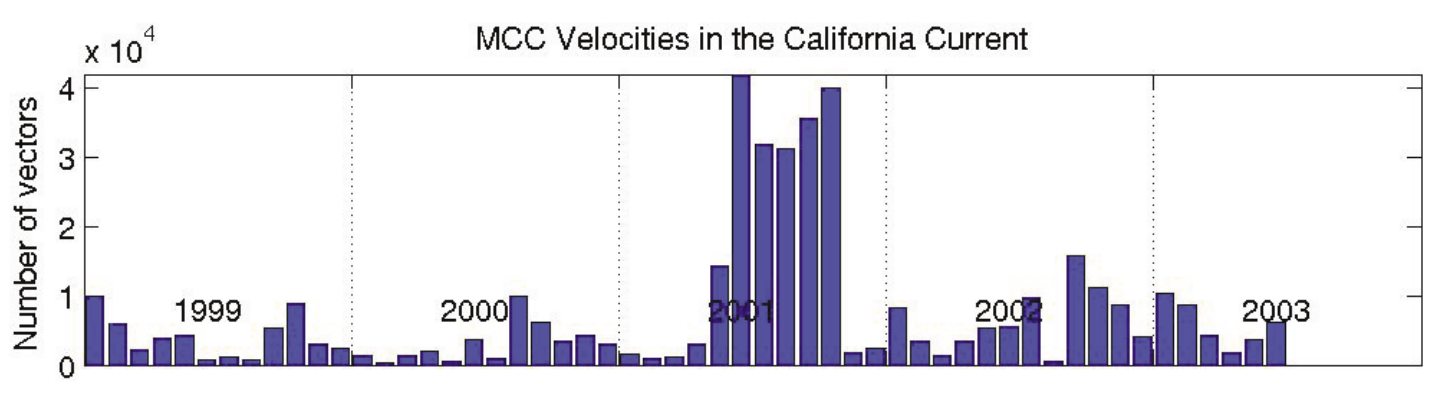

Compared with altimetry derived currents, surface velocities derived by tracking features in thermal imagery using the MCC method (see far left) have finer temporal and spatial sampling due to more frequent measurements by AVHRR platforms and the ability of the MCC method to track patches 22 kilometers in size. This method is most effective during time periods with low cloud cover and near the coast where the thermal gradient is high (see above).

OI Results and Statistics

Two separate series in time are shown (see below): the first in January, a relatively cloudy month for the region, and the second in July, a somewhat cloud-free month (see # of vectors per month above). For each series, five OI's are given: Topex alone, Topex plus ERS, Topex plus ERS and GFO, MCC alone, and a combined OI with all three altimeters merged with the MCC vectors. During the January series the 3 altimeters pick up most of the flow in the fully merged OI, showing how essential altimetry is during periods of extensive cloud cover. However during July, the three-altimeter configuration does not pick up several main features evident in the MCC OI or the combined OI. This is due to the fact that along track only measurements of sea surface height enables only the cross track component of the surface geostrophic velocity to be computed. To further demonstrate differences in spatial resolution, normalized error maps and two dimensional wavenumber spectra for the U-component (east-west) are given for each OI. The calculation of the wavenumber spectra required a rectangular area with no land present. The northern limit of this rectangle is 37˚ N, the southern limit is 32˚ N, the eastern limit is 122˚ W, and the western limit is 130˚ W. The normalized error maps illustrate how the addition of each altimeter can greatly reduce the amount of error in each OI. During cloudy periods, the three-altimeter configuration results in less error than 10 days of MCC vectors. A comparison of the spectral figures, however, show that the altimeters undersample mesoscale features when compared with the MCC, for both cloudy and less cloudy periods.

Next Steps

Future work will focus on verifying the OI velocities using direct observations in the region. Also, we will be merging the sst imagery with ocean color from the Moderate Resolution Imaging Spectroradiometer (MODIS). Ocean color is dominated by advection and often produces results at times and places where thermal gradients are weak. In all, 12 years of AVHRR images will be merged with all available altimetry and color data in the California Current region.

References

Bowen MM, WJ Emery, JL Wilken, PC Tildesler, IS Barton, and R Knewtson, 2002: Extracting multi-year currents from sequential imagery using maximum cross-correlation technique, J. Atmos. Oceanic Tech., 19, 1665-1676.
LeTraon, KA, and PT Strub, 1992: Mapping the oceanic mesoscale circulation: validation of satellite altimetry using surface drifters, J. Atmos. Oceanic Technol., 9, 687-698.
Wilken JL, MM Bowen, and WJ Emery, 2002: Mapping mesoscale currents by optimal interpolation of satellite radiometer and altimeter data, Ocean Dynamics, 52, 93-103.